

# Screening of ten different plants in the process of supercritical water gasification

Julian Dutzi<sup>\*</sup>, I. Katharina Stoll, Nikolaos Boukis, Jörg Sauer

Institute of Catalysis Research and Technology (IKFT), Karlsruhe Institute of Technology (KIT), Eggenstein-Leopoldshafen, 76344, Germany

## ARTICLE INFO

### Keywords:

Supercritical water  
Biomass  
Hydrogen  
Homogeneous catalyst

## ABSTRACT

It is important to know the limitations of the supercritical water gasification (SCWG) in terms of behavior of different biomasses, especially when determining whether SCWG is a suitable conversion process for a certain biomass. Ten different biomasses (eight different plant species, of which two were grown in two different sites) were processed to evaluate this aspect. Moist and dry, woody and grassy biomasses were gasified in the same experimental setup under similar conditions. Only small differences could be seen in the gasification experiments. The carbon gasification efficiency was  $60.3 \pm 5.1\%$ , the gas compositions were very similar. Solid deposits formed in all experiments in the same temperature zone of the reactor containing coke, salt building elements and heavy metals, sometimes leading to plugging. Nevertheless, an experimental duration of 6 h could be achieved for the dry biomasses. The experiment with the moist biomass Reed Canary Grass was ended early due to plugging of the feed tubing which is due to the different size reduction procedure for moist biomasses resulting in bigger biomass particles. This emphasizes the importance of sufficient size reduction prior to the experiment. Potassium addition as a homogeneous catalyst, in form of potassium hydroxide, has proven to be beneficial regarding gasification efficiency, but poses a threat regarding plugging due to salt deposits in the system.

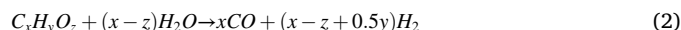
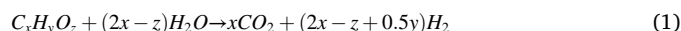
## 1. Introduction

Cleaning of contaminated soils, groundwater and air is important due to the threat that they pose to animals, humans and the environment [1]. Phytoremediation is a technology to clean the soil, groundwater and air by the use of plants [2]. Within the EU H2020-project CERESiS (“Contaminated land Remediation through Energy crops for Soil improvement to liquid fuel Strategies”) the phytoremediation of contaminated soils is investigated [3]. The main focus lies on the remediation of heavy-metal contaminated soils. The plants that are used for phytoremediation are subsequently contaminated and need to be treated in some way in order to avoid secondary contamination [4–6]. Within CERESiS the conversion of these plants in the processes of Fast Pyrolysis (FP) and Supercritical Water Gasification (SCWG) is assessed.

SCWG is an innovative technology that utilizes water as a reaction medium to efficiently convert biomass into gaseous products. SCWG operates at high temperatures ( $T > 374\text{ °C}$ ) and pressures ( $p > 221\text{ bar}$ ), creating a supercritical state of water. This state allows for exceptional miscibility with the organic feedstock due to the non-polar character of

supercritical water, promoting rapid and homogeneous reactions, making it a highly effective process for biomass conversion [7].

In the supercritical water, the biomass molecules undergo hydrolyzation and are subsequently further decomposed, according to the model reactions Eqs. 1 and 2. The produced gaseous species react according to the Water-Gas-Shift (WGS) reaction (Eq. 3) and to the methanation reactions (Eqs. 4 and 5) [8–11].



Typically, the gas generated through SCWG is predominantly composed of  $H_2$ ,  $CH_4$  and  $CO_2$ , with smaller amounts of  $C_2$  and  $C_3$  compounds and  $CO$  [12–15]. Considering the global efforts towards

<sup>\*</sup> Corresponding author.

E-mail address: [Julian.Dutzi@kit.edu](mailto:Julian.Dutzi@kit.edu) (J. Dutzi).

cleaner and more sustainable energy sources, the production of hydrogen from biomass using SCWG has obtained significant attention. Hydrogen is considered a clean fuel crucial for facilitating the transition from fossil fuels to renewable energy sources [16]. The product gas can be further upgraded via steam reforming of the produced hydrocarbons to increase the H<sub>2</sub> yield [17]. SCWG provides a promising pathway for sustainable hydrogen production, utilizing organic biomass resources and minimizing greenhouse gas emissions.

As described above, in the framework of the EU-project CERESiS the focus lies on the phytoremediation of contaminated soil around the globe. As different biomasses can be grown in different parts of the world due to limitations like climate or soil quality, it is important to investigate whether there are major differences between different biomasses regarding the downstream processing via SCWG. For this purpose, continuous SCWG experiments were conducted with biomasses from different regions of the world (England, Italy and Brazil) in the framework of the current study. In addition to the investigation of the processability, the influence of potassium addition as a homogeneous catalyst, in form of potassium hydroxide, on the process with biomasses relevant for the CERESiS project was assessed.

## 2. Materials and methods

### 2.1. Preparation of educts

Ten different biomasses were used (eight different plant species of which two plants were evaluated from two different growing sites) (see Fig. 1 and Table 1).

They were provided by the CERESiS partners from Scotland, Italy and Brazil in various forms. The biomasses Silvergrass (lat. *Miscanthus*) and Short rotation coppice were grown in two different locations in England, abbreviated with ST and HH. The dry biomasses (DM > 90 wt %) had to be milled to a size of 0.25 mm or smaller. Biomasses E, F, G and J (see Fig. 1) were milled prior to delivery. The size of biomasses A, B, C and D was reduced by a mill with a 0.2 mm sieve (Pulverisette 14, Fritsch GmbH). For biomass I (wooden stems and branches of grapevines) two preliminary size reduction steps were carried out: first in a wood chipper (GE 260, Viking GmbH) to about 2 cm long pieces, then in a mill with 4 mm sieve (Pulverisette 25, Fritsch GmbH).

Biomass H (RCG) was provided in moist form (DM = 54.2 wt%). The size was reduced by a meat grinder, as a mill was not sufficient due to the high water content. In different size reduction steps (see Fig. 2) the size was reduced below 1 mm. A size analysis has not been performed. Fig. 3.

The reduced size biomass H can be seen in Fig. 2. The biomass is not in the form of powder and displays small fibers. Except for the different size reduction pathways, the further feed preparation was carried out in

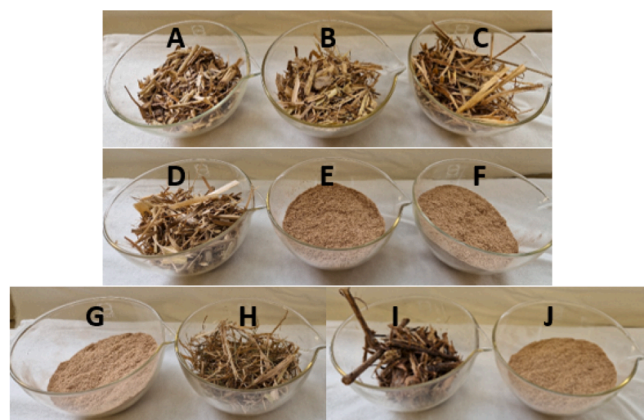


Fig. 1. Pictures of biomasses as received from project partners (A: PV; B: AD; C: EC; D: SC; E: ST-MC; F: HH-MC; G: ST-SRC; H: RCG; I: GV; J: HH-SRC; for abbreviation see Table 1).

Table 1  
Labeling of biomasses in the current study.

English name	Latin name	Abbreviation in the following text
Switchgrass	<i>Panicum virgatum</i>	PV
Giant Reed	<i>Arundo donax</i>	AD
Grapevine	<i>Vitis vinifera</i>	GV
Silvergrass	<i>Miscanthus</i>	MC (either grown in HH or in ST)
Short rotation coppice	–	SRC (either grown in HH or in ST)
Reed Canary Grass	<i>Phalaris arundinacea</i>	RCG
Sugar Cane	<i>Saccharum officinarum</i>	SC
Energy Cane	–	EC



Fig. 2. Inner setup of meat grinder and size reduced Reed Canary Grass (RCG) (Biomass H).

the same way.

The feed slurry was created by adding distilled water to the biomass powder in such a ratio that a dry matter content of 8 wt% was achieved. Xanthan, provided by Carl Roth GmbH, was added as a thickening agent (0.5 wt%) to prevent phase separation, and KOH (5000 mg K<sup>+</sup>/kg feed slurry, if not stated otherwise in the text), provided by Merck KGaA, was added as a homogeneous catalyst. After the addition of the additives the feed was thermally pretreated at T = 70 °C in a mixer for two hours under constant stirring (Thermomix TM31, Vorwerk Deutschland Stiftung & Co. KG).

Additionally, in four experiments methanol, provided by Merck KGaA, was added to the feed slurry (2 wt% methanol). With the addition of methanol, that is easily decomposed under supercritical conditions, the influence of a hydrogen donor on the gasification efficiency and the suppression of coke formation in the system was investigated, as described in Section 2.1.

Before every experiment with the CERESiS biomasses pre-experiments were carried out with ethanol solution (5 wt% ethanol). The ethanol was supplied by VWR Chemicals. These pre-experiments were conducted to reach a gas-liquid-equilibrium in the system prior to feeding the biomass. With this procedure dead volumes in the lab-plant are filled with a water phase and gases with very similar composition like the later experiment and steady-state operation can be reached more quickly during the main experiment.

### 2.2. Apparatus

The experiments are carried out in the continuous SCWG-plant LENA (German acronym for “Laboratory Plant for Energetic Utilization of Agricultural Materials”). It can be operated at T ≤ 700 °C and p ≤ 300 bar. In the present configuration the LENA plant consists of two main parts: a preheater and SCWG reactor. The preheater is made of a 750 mm long SS316 pipe (9/16 in. outer diameter, 8 mm inner diameter). The pipe is heated from the outside by two spiral heaters. Temperatures are monitored by six thermocouples on the outside of the pipe. After the feed is preheated to about 350 °C it enters the gasification reactor which is made of the nickel-base alloy 625 and has a length of 1500 mm (9/16 in. outer diameter, 8 mm inner diameter). Seven spiral heaters and 21 thermocouples are mounted on the outside of the pipe. In the reactor the main reactions between organics and water take place to form mainly gaseous products.

Downstream of the reactor a filter bearing (F01) is installed to collect

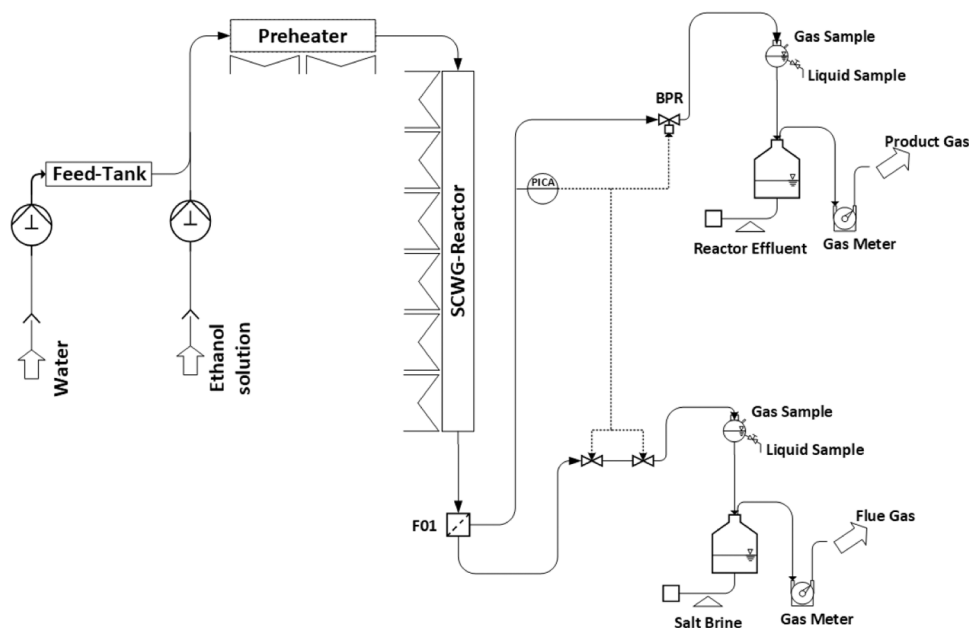


Fig. 3. Process scheme of the LENA plant in the current configuration.

solids and tars that formed in the process. Salts that precipitated in the supercritical state of water (in the gasification reactor) might re-dissolve in the cooled water in the filter bearing. The formed salt brine can be retracted from the sump of the filter bearing by a two needle-valves, that open shortly after each other (20 ms) and act as a sluice. They open every 5 min and separate about 3 ml of salt brine into a glass container. The product gas and the reactor effluent leave the filter towards the back-pressure regulator (BPR) provided by Tescom. After the BPR follows the phase separation. Gas and liquid samples can be collected and analyzed. The products are quantified using scales and gas meters.

To start up the experiment the system is pressurized with water using a high-pressure pump by Prominent and subsequently heated. To reach a gas-liquid-equilibrium in the system ethanol solution is gasified prior to feeding the biomass. With this procedure steady-state operation can be reached faster during the main experiment. The ethanol solution is fed into the system by a HPLC pump during the night before the experiment with biomass. For the biomass experiment the feed slurry is stored in a pressurized tank. A water-driven piston pumps the feed into the system in defined amounts (for details see [18]). Pressure, flow and temperatures are set and monitored in the process control system.

### 2.3. Analysis

The gas samples obtained from the product gas are subjected to immediate analysis using the gas chromatograph 5890 series II plus (Hewlett-Packard GmbH), equipped with a fused silica capillary column (Carboxen 1010 PLOT 30 m, SUPELCO). The thermal conductivity and flame ionization detectors are utilized to determine the volume fractions of gas components, namely H<sub>2</sub>, CO, CH<sub>4</sub>, CO<sub>2</sub>, C<sub>2</sub>H<sub>4</sub>, C<sub>2</sub>H<sub>6</sub>, C<sub>3</sub>H<sub>8</sub> and C<sub>3</sub>H<sub>6</sub>. Gas samples are collected in 30-minute intervals.

Throughout the experiment, small liquid samples are regularly collected from the effluent streams. The remaining effluent streams are collected in a glass container, forming the total effluent. The Total Carbon (TC) content in both liquid samples and total effluent is determined through combustion, while Total Inorganic Carbon (TIC) is extracted through acid extraction in a TOC analyzer (DIMATOC 2100, DIMATEC Analysentechnik GmbH). Total Organic Carbon (TOC) is then calculated by subtracting TIC from TC. The concentration of trace elements, such as Al, Ca, Cr, Cu, Fe, K, Mg, Mo, Na, Ni, S, Si, and Zn, is determined using ICP-OES (Inductively Coupled Plasma-Optical

Emission Spectrometry) with an Agilent 725 spectrometer (Agilent Technologies).

For the analysis of solid samples, SEM-EDS (Scanning Electron Microscope-Energy Dispersive X-ray Spectroscopy) is performed using a GeminiSEM 500 instrument (Carl Zeiss AG).

### 2.4. Data interpretation

To interpret the acquired data the carbon efficiency CE and the TOC-conversion are calculated, using data from steady state operation. Steady state is achieved once gas amount and gas composition are constant. This is ensured by frequent measurement of these variables, as described in Section 2.3.

Carbon Efficiency (CE) quantifies the fraction of carbon present in the feed that undergoes transfer to the gas phase during gasification. It serves as a significant indicator, describing the effectiveness of converting organic components within the feed solution into gaseous products. The properties of these gases are estimated using the ideal gas law. CE is calculated as follows:

$$CE = \frac{\sum \beta_i * x_i * \frac{V_{Gas,p}}{R * T} * M_c}{\dot{m}_{Feed} * \alpha} \quad (6)$$

$x_i$  Concentration of component 'i' in the gas product (vol%).

$\alpha$  Carbon concentration in the feed (wt%).

$\beta_i$  Number of carbon atoms of component 'i' in the gas product.

$\dot{m}_{Feed}$  Feed mass flow (g/h).

$M_c$  Molar mass of carbon (g/mol).

$p$  Pressure (Pa).

$R$  Universal constant of gases (J/(mol\*K)).

$T$  Temperature (K).

$V_{Gas}$  Gas flow under ambient conditions (l/h).

TOC-conversion quantifies the fraction of Total Organic Carbon (TOC) present in the feed slurry that undergoes conversion into various forms, gases, dissolved inorganic compounds, and organic residues such as coke, tar, and soot. This conversion figure serves as a significant indicator, providing insights into the quality of the wastewater. The TOC-conversion is defined as follows:

$$TOC_{conv} = 1 - \frac{\dot{m}_{R,effluent} * TOC_R + \dot{m}_{S,effluent} * TOC_S}{\dot{m}_{Feed} * \alpha} \quad (7)$$

$\dot{m}_{R,effluent}$  Mass flow of reactor effluent (g/h).

$\dot{m}_{S,effluent}$  Mass flow of salt concentrate (g/h).

$TOC_R$  TOC content of liquid 'i' (mg/g).

$TOC_S$  TOC content of salt concentrate (mg/g).

To assess the deviation of the results the mean value  $\mu$  and the standard deviation  $\sigma$  are calculated according to Eq. 8 and eq. 9.

$$\mu = \frac{1}{n} \sum_{i=1}^m x_i \quad (8)$$

$$\sigma = \sqrt{\frac{\sum_{i=1}^m (x_i - \mu)^2}{n}} \quad (9)$$

n Number of values considered (-).

$x_i$  Value of sample i (%).

### 3. Results and discussion

The SCWG experiments were conducted with a reaction temperature of 650 °C and a pressure of 280 bar. Higher temperatures would be beneficial regarding CE and TOC conversion [19–21] but due to limitations of the used reactor material are not possible. The pressure was chosen out of experience. Generally, a change in pressure does not have significant influence on CE, as shown in [20,22]. The biomass content in the feed slurry was 8 wt% and the flow rate was set to 200 g h<sup>-1</sup>. The set temperature profile can be seen in Fig. 4. The set temperature profile resulted in a 900 mm long zone in which the temperature was greater than 600 °C (relevant for gasification; mean residence time in this zone was 65 s).

#### 3.1. Influence of the addition of potassium hydroxide and methanol to the biomass slurry on the gasification efficiency

The influence of hydrogen that is present in the reaction system on the coke formation during the gasification of biomass was investigated by adding methanol to the feed slurry. Methanol is a molecule that can easily be gasified under the conditions of SCWG [22–24]. Boukis et al. found that methanol is completely gasified at temperatures of 600 °C and decomposition is already measurable at temperatures of 400 °C [22]. In the process of methanol gasification hydrogen is formed early in the system. The present hydrogen could inhibit coke formation as already described in other processes like mild pyrolysis [25] or oil upgrading [26] where hydrogen is introduced to reduce coke formation. In hydrothermal liquefaction hydrogen introduction to the system by either directly feeding it [27] or by feeding a hydrogen donor like methanol [28] or tetralin [29] decreased coke formation noticeably. Even though coke formation is generally reduced in the environment of SCWG due to the high water surplus and thus low contact rates of

biomass molecules [30,31] it cannot be neglected as prior work shows [18]. In comparison, in experiment 5 no methanol was added (see Table 2).

The influence of the added methanol is assessed by comparing experiment 5 (no methanol, 5000 ppm K<sup>+</sup>) and experiment 4 (2 wt% methanol, 5000 ppm K<sup>+</sup>). When comparing the CE, experiment 4 displays a 7% higher CE (see Table 2). The gas composition is very different, as shown in Fig. 5. Much more hydrogen is present in the system during experiment 4, as expected from the gasification of methanol.

To evaluate whether PV was gasified better in presence of methanol (less carbon deposits), the CE of experiment 4 is corrected by the gasified amount of carbon that originates from methanol. Methanol can be considered completely gasified under the present conditions [22]. When correcting CE to only the carbon originating from PV, CE is 69.8 % and thus nearly the same as during experiment 5.

From these results it can be concluded that more hydrogen is present in the system when methanol is added to the feed, as displayed in Fig. 5. With 2 wt% methanol this amount of hydrogen is either not enough to suppress coke formation or the idea of introducing hydrogen to the system to reduce coke formation is not valid in case of SCWG. Either way further investigation with higher concentrations of methanol or other easy to decompose substances should be conducted in the future.

Secondly, the influence of alkaline catalysts on the process of SCWG was investigated. Ions of alkaline metals are known as homogenous catalysts in the process of SCWG [32,33]. They increase the gasification efficiency and catalyze the WGS shift reaction, thus increase the hydrogen content of the product gas [11,34]. This has been described in experiments with the biomass model compound glucose by Sinag et al. [35]. They were able to significantly increase the H<sub>2</sub> yield. D'Jesus found that the addition of potassium in form of KHCO<sub>3</sub> increased the gasification efficiency during corn starch gasification from 82 % (0 ppm K<sup>+</sup>) to 92 % (500 ppm K<sup>+</sup>) [20]. Additionally, alkaline metals in form of KOH or NaOH weaken the intermolecular bond between biomass macromolecules due to their alkaline character [36]. Thus, these macromolecules are easier to break and thus gasify.

A downside of the addition of the alkaline metals is that they form solid salts in the process that can precipitate [37–39] and can cause

**Table 2**

Experiments varying K<sup>+</sup> concentration and methanol addition (T<sub>Reaction</sub> = 650 °C, p = 280 bar).

Exp. Nr.	Methanol / wt%	K <sup>+</sup> / ppm	CE / %	TOC conversion / %
1	2	0	61.0	94.8
2	2	1000	64.8	95.1
3	2	3000	63.3	96.0
4	2	5000	75.0	95.0
5	–	5000	68.0	94.8

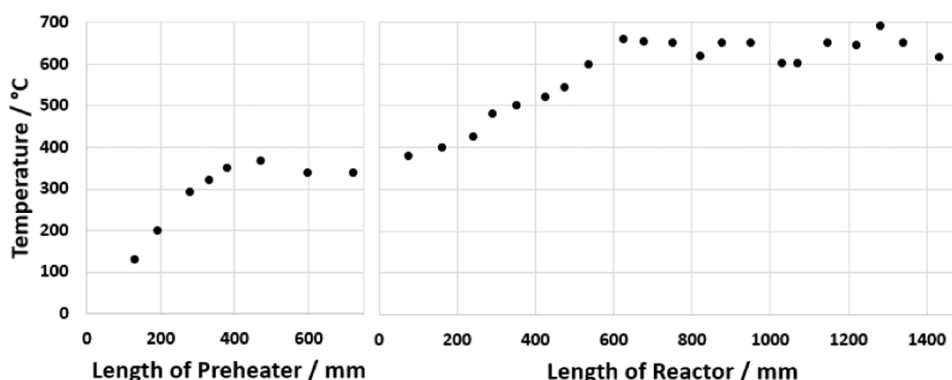


Fig. 4. Outside temperature profile, representative of the conducted experiments.

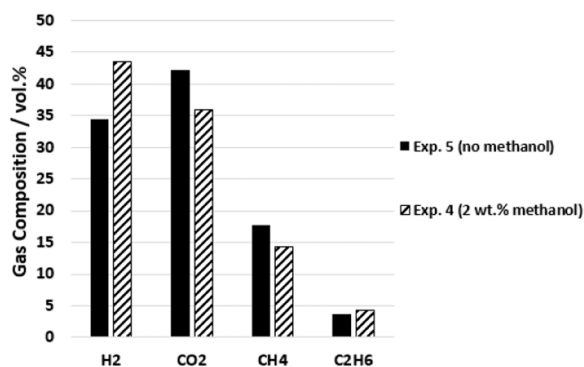


Fig. 5. Gas composition without and with addition of methanol ( $T_{\text{Reaction}} = 650\text{ }^{\circ}\text{C}$ ,  $p = 280\text{ bar}$ ).

blockage of the flow and blockage of the flow [21,40]. This has also been reported by the authors' previous publication [18].

To investigate the influence of potassium on the biomass PV, the potassium concentration was varied between 0 and 5000 ppm (see Table 2). Potassium was present in the feed in form of KOH. The biomass slurry was thermally pretreated at mildly elevated temperatures [41,42] (a temperature of  $70\text{ }^{\circ}\text{C}$ ) in a mixer after the addition of KOH to enable alkaline hydrolysis. Additionally, 2 wt% of methanol was added in experiments 1, 2, 3 and 4.

The conducted experiments displayed that the gasification efficiency increased from 61 to 75 % with increasing potassium concentration from 0 to 5000 ppm (see Fig. 6). Since the gas volume increased and the TOC conversion of these experiments was the same (as displayed in Table 2), it can be assumed that less coke formed in the process. This possibly originates from the alkaline pretreatment which enables easier splitting of the biomass molecules. This assumption is supported by the duration of the experiments which is limited by the formation of solid deposits and thus by plugging of piping. While a duration of 8 h was the set goal, only the experiments with 3000 and 5000 ppm  $\text{K}^+$  were able to reach it. The experiment without added  $\text{K}^+$  ended after 7 h and the experiment with 1000 ppm  $\text{K}^+$  after 6.5 h due to plugging of the gasification reactor. The experiments with higher concentrations also showed deposits after opening the reactor but to a smaller extend.

The gas composition was also influenced by the addition of KOH (see Fig. 7). The amount of hydrogen increased from 44 to 50 vol% when the potassium concentration was increased from 0 to 3000 ppm. As the produced amount of gas simultaneously increased from 1.02 to 1.15  $\text{Nl}_{\text{dry matter}}^{-1}$  the absolute hydrogen amount produced increased as well. At 5000 ppm  $\text{K}^+$  the hydrogen content decreased. This might be an outlier, since the WGS is catalyzed by potassium and thus the  $\text{H}_2$  should have further increased [35]. The WGS should also increase the  $\text{CO}_2$  concentration in the product gas according to Eq. 3. This is not the case in the present experiments. A possible reason for this could be the increased formation of  $\text{KHCO}_3$  or  $\text{K}_2\text{CO}_3$  with increasing amount of  $\text{CO}_2$  present, according to Eq. 10 [43].

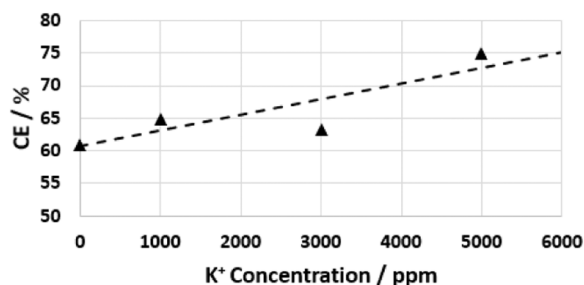


Fig. 6. Carbon Efficiency (CE) in dependency on potassium concentration in the feed with 2 wt% methanol in the feed ( $T_{\text{Reaction}} = 650\text{ }^{\circ}\text{C}$ ,  $p = 280\text{ bar}$ ).

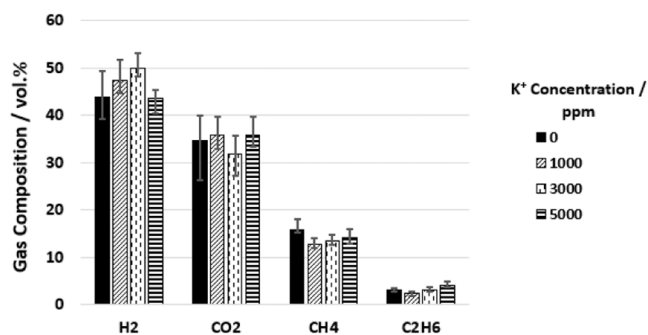


Fig. 7. Gas composition in dependency on potassium in the feed (with indication of maximal and minimal value) ( $T_{\text{Reaction}} = 650\text{ }^{\circ}\text{C}$ ,  $p = 280\text{ bar}$ ).



In all cases the pH value dropped from  $\text{pH} = 9.3 \pm 0.1$  in the feed to a  $\text{pH} = 6.5 \pm 0.3$  in the reactor effluent. Thus, most of the potassium is presumably not present in form of KOH anymore.

Potassium is not known to enhance the methanation reaction [44]. Thus, the methane content is relatively stable. The ethane content slightly increases with increasing potassium in the feed. This might be due to the better splitting of the macromolecules due to the alkaline character [36].

As stated at the beginning of this section a downside of the addition of alkaline metals is the formation of salts that can possibly deposit and thus need to be removed from the mixture at some point [45,46]. Once supercritical temperatures are reached salts are beginning to precipitate due to decreasing solubility. Salts are separated in two groups, type 1 and type 2 salts [38,39,45]. Type 2 salts are poorly soluble in supercritical water (e.g.  $\text{K}_2\text{SO}_4$ ) while type 1 salts only begin to precipitate at further elevated temperatures (e.g.  $\text{K}_2\text{CO}_3$ ) [37,45]. The precipitating salts can cause corrosion at  $T > 500\text{ }^{\circ}\text{C}$  [30,47–49] and blockage of the flow as described by Dutzi et al. [18]. A salt separation was not performed prior to the reactor. A filter bearing was installed after the gasification reactor to collect precipitated salts that were transported downstream. A salt separation prior to the gasification reactor would increase the complexity of the lab-plant, as the arrangement of preheater and reactor would need to be changed. An additional salt separation device would need to be implemented in the hot part of the reaction system. This could lead to leakages, as the number of screw connections increases. Additionally, such a salt separation would also separate part of the organic matter of the preheated feed and thus decrease the amount of gasifiable carbon. Possible benefits would be the reduced risk of solid deposits in the reactor if the salt separation work sufficiently. To implement such a salt separation is possible, as shown in [18]. For the present study of the influence of biomasses it was chosen not to implement a salt separation prior to the gasification reactor to keep the

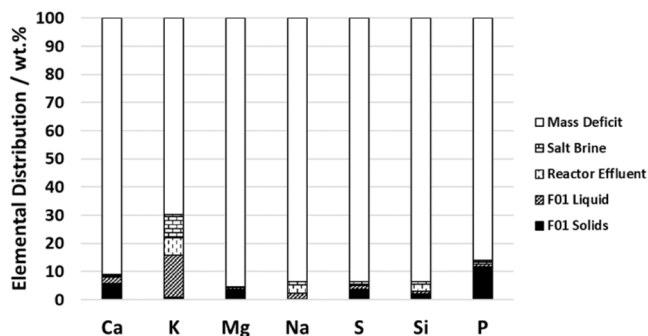


Fig. 8. Distribution of salt building elements in the products for experiment 2 (1000 ppm  $\text{K}^+$  added) ( $T_{\text{Reaction}} = 650\text{ }^{\circ}\text{C}$ ,  $p = 280\text{ bar}$ ).

process as simple as possible.

In Fig. 8 the distribution of salt building elements in the product fractions is displayed for experiment 2. For all elements the mass balance is poor, at maximum 30 wt% of the fed masses can be detected in the products. Possible reasons for this can be dilution of the salt building elements in liquid effluents below detection limits and also the formation of solid deposits in the system. These solid deposits that were not transported to the filter bearing and stayed in the gasification reactor cannot be collected to analyze them quantitatively. Thus, in general a salt separation prior to the gasification reactor is recommended, as the salt do not reach the filter after the gasification reactor.

Since the salt separation is very poor and most salt building elements remain in the system, especially potassium poses a threat to plugging the reactor, as the mass that stays in the system is the highest of all salts due to the addition of KOH as homogeneous catalyst. In all experiments where KOH was added the mass balance was not complete, as shown in Fig. 9. In case of no added KOH, 60 wt% of the potassium in the biomass could be detected in the products. The worst mass balance appeared in case of 1000 ppm  $K^+$ . The more potassium was added into the feed the better the mass balance was due to an increased amount of potassium leaving the system in form of reactor effluent, either detected in the reactor effluent or in the filter of the reactor effluent. Almost no potassium deposited into the salt brine collected at  $T < 100$  °C. Even though the mass deficit decreased with increasing amount of KOH added, the absolute amount of potassium that remained in the system increased as shown in Table 3 when processing the same amount of feed. In order to avoid excessive deposits, the potassium concentration was not further increased beyond 5000 ppm.

### 3.2. Influence of the biomass type on the gasification in SCWG

SCWG is supposed to be able to process a wide variety of biomasses, either moist or dry. In literature it has been reported that kitchen waste, animal manure, sewage sludge, dry plants and many more biomasses have been gasified [21,50–52]. For example, D'Jesus et al. found that corn silage and clover grass were equally gasified and produced similar product gases [32]. Dutzi et al. have previously gasified two different dry biomasses (Reed Canary Grass and grapevines) and found that they behaved similarly in the system [18]. It is important to understand the influence of the biomass on the process of SCWG. In the case of CERESiS, it must be known if some plants need to be excluded for the phytoremediation because a subsequent processing in SCWG would not be possible. For this purpose, ten different biomasses were evaluated under the same conditions. The feed was prepared according to Section 2.1. The biomasses are listed in Table 4. They are very similar in composition, e.g. the carbon content is for example  $45.0 \pm 2.0$  wt%. The appearance though is very different (as displayed in Fig. 1). The biomass GV for example is a woody biomass while MC is a grass. Thus, in these experiments a wide range of differently structured plants is covered.

The experiments displayed quite similar results. The mean CE is 60.3

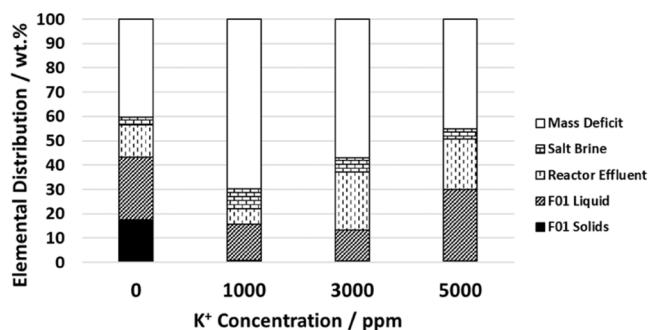


Fig. 9. Potassium distribution in products during experiments with different potassium concentrations in the feed ( $T_{\text{Reaction}} = 650$  °C,  $p = 280$  bar).

Table 3

Amount of potassium remaining in the system.

Added $K^+$ / ppm	0	1000	3000	5000
$K^+$ in Feed / ppm	180	1110	2940	5050
Mass Deficit / %	40.3	69.8	56.9	45.1
Mass Deficit / ppm	72.5	774.9	1674.0	2275.3
Mass remaining in system* / g	0.15	1.55	3.35	4.55

\* when 2 kg of feed were pumped into the system

Table 4

Dry Matter (DM) content of biomass and elemental analysis (CHNO) based on dry matter (in wt%).

Exp. Nr.	Biomass	DM	C	H	N	O
5	PV	97.7	43.6	6.4	0.4	46.8
6	SC	92.8	43.2	6.0	0.7	n.d.
7	AD	95.5	43.1	6.4	0.4	46.2
8	GV	95.1	47.1	4.5	1.2	47.2
9	ST-MC	99.4	45.9	6.9	0.8	40.7
10	ST-SRC	100.0	47.7	7.4	0.5	42.3
11	HH-MC	99.6	45.2	6.8	0.5	41.3
12	HH-SRC	100.0	48.2	7.0	0.6	42.1
13	RCG	54.2	43.7	9.2	1.3	45.8
14	EC	93.5	42.4	6.1	0.7	n.d.
	Mean $\mu$		45.0	6.7	0.7	44.1
	Standard deviation $\sigma$		2.0	1.1	0.3	2.5

\*n.d. = not determined

% with a standard deviation of 5.1 % (as can be seen in Table 5). The ability to gasify the different plants was thus similar. Regarding the gasification efficiency no differences was detectable between moist biomass like RCG (CE = 59.4 %) and the dry biomasses (mean CE of dry biomasses  $\mu = 60.4 \pm 5.4$  %). Thus, the ability to gasify biomasses does not seem to depend on the degree of humidity of the biomass. Seemingly, biomasses with similar elemental composition (see Table 4), if moist or not, if woody or grassy, can similarly be gasified. Assuming Gaussian distribution of the CE of similar biomasses, a typical significance interval ( $\pm 2\sigma$ ) can be set (see Fig. 10). With this tool, future biomasses can be evaluated regarding the ability to gasify them. In case the CE lies inside the significance interval no significant deviation can be detected. If for example, calculating the mean and standard deviation without considering the biomass EC (i.e. prior to the last experiment) it becomes clear that the gasification of EC falls into this interval and thus is not significantly different from the other results.

When visualizing the gas compositions (Table 5) in box plots (see Fig. 11) it becomes clear that the gas compositions of the gasification of different biomasses are quite similar. The variance in  $C_2H_6$  content ( $3.8 \pm 0.7$  vol%) and in  $CH_4$  content ( $16.9 \pm 1.8$  vol%) is very low. In  $H_2$  content and  $CO_2$  content more variance is visible.  $33.5 \pm 3.2$  vol% of  $H_2$  are formed. In case of RCG (moist biomass) most hydrogen formed

Table 5

Carbon Efficiency (CE) and gas composition of different biomass experiments under same conditions.

Exp. Nr.	Biomass	CE %	$H_2$ vol%	$CH_4$ vol%	$CO_2$ vol%	$C_2H_6$ vol%
5	PV	68.0	34.4	17.7	42.3	3.8
6	SC	55.0	37.3	17.7	39.8	3.7
7	AD	68.2	33.9	19.6	39.4	4.9
8	GV	53.2	35.2	16.7	43.4	3.4
9	ST-MC	60.4	27.9	16.6	48.8	4.5
10	ST-SRC	65.1	32.3	19.2	42.1	4.3
11	HH-MC	55.6	31.7	17.3	44.7	4.1
12	HH-SRC	57.0	30.3	13.2	52.6	2.6
13	RCG	59.4	39.7	15.0	41.6	2.5
14	EC	60.7	32.7	16.2	45.6	3.9
	Mean $\mu$	60.3	33.5	16.9	44.0	3.8
	Standard deviation $\sigma$	5.1	3.2	1.8	3.9	0.7

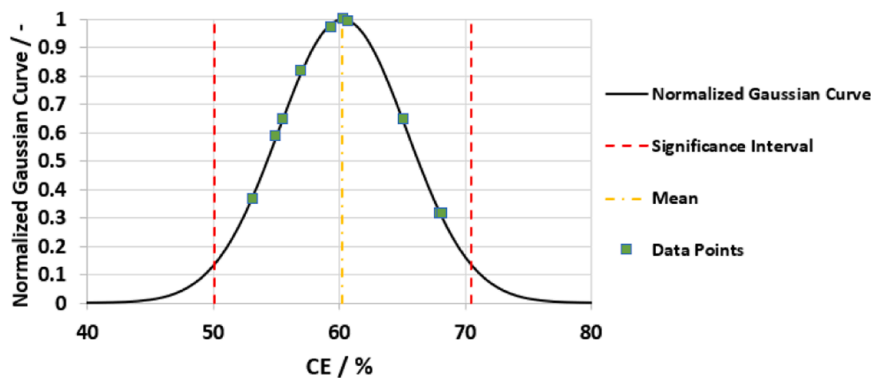


Fig. 10. Carbon Efficiency (CE) of different biomass experiments in Gaussian curve ( $T_{\text{Reaction}} = 650\text{ }^{\circ}\text{C}$ ,  $p = 280\text{ bar}$ ).

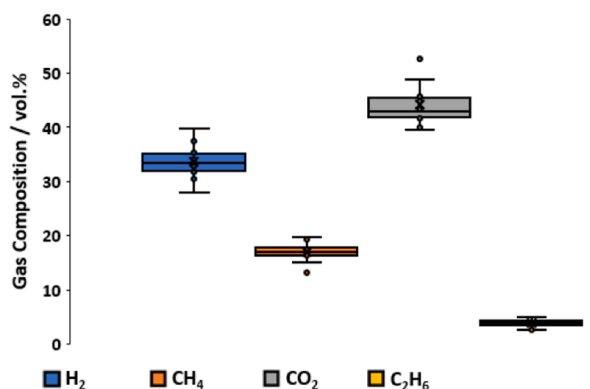


Fig. 11. Gas compositions of different biomasses ( $T_{\text{Reaction}} = 650\text{ }^{\circ}\text{C}$ ,  $p = 280\text{ bar}$ ).

(39.7 vol%). This might be due to the fact that RCG shows a higher hydrogen content in the dry biomass (see Table 4). Possibly it is also beneficial to feed the biomass in moist form to generate more  $\text{H}_2$ . In case of  $\text{CO}_2$ ,  $44.0 \pm 3.9\text{ vol}\%$  are formed. HH-SRC showed deviations in the  $\text{CO}_2$  and  $\text{CH}_4$  content (outliers in Fig. 11).

One significant difference appeared in the gasification of moist and dry biomass. The experiments with dry biomass all lasted at least 6 h prior to clogging, except for the biomass GV, but this must have been an outlier as Dutzi et al. showed that this biomass is equally gasified as grasses with similar elemental composition [18]. With RCG, which was the only biomass processed in moist form, the experiment ended after 3 h but not due to formation of solid deposits in the reaction system but

due to blocking of the feed tubing. As described in Section 2.1, RCG was ground up with a meat grinder to a size smaller than 1 mm. As the feed tubing has an inner diameter of 2.5 mm this size reduction was not sufficient. In future experiments with moist biomasses a different size reduction approach needs to be chosen.

As described above the gasification efficiency is far from 100%. Some carbon remained in the reactor effluent, but only in small amounts ( $\text{TOC}_{\text{effluent}} = 2000 \pm 510\text{ ppm}$ ). Since the  $\text{TOC}$ -conversion was  $95.3 \pm 0.8\%$  in all cases and almost no TIC was detectable most of the carbon that did not form gaseous products deposited in some way. Additionally, tarry material formed that could not be quantified. After all experiments solid deposits were found in the gasification reactor about 50 cm from the top (set temperature on the outside  $500\text{ }^{\circ}\text{C}$ ). In some cases, these deposits led to blockage of the flow and thus to an early end of the experiments. Dutzi et al. described this phenomenon in detail based on Reed Canary Grass and grapevines [18]. They found that these deposits consist of coke and salts that precipitate in the process. This can be confirmed by the EDS-analysis of solid deposits that were mechanically removed from the gasification reactor after these experiments (see Table 6). The solids in the reactor mainly consisted of carbon and secondly of salt building elements like Si, K and Ca. Not all solids deposited in the gasification reactor, in some cases the solids also dropped into the filter bearing below the reactor. These solids were also collected and analyzed via EDS. The analysis is shown in Table 7. It can be seen that also most of these solids are made of carbon in form of coke. In some cases, salt building elements like K (experiments 7, 9 and 11) or Si (experiments 11 and 13) are predominant. In experiments 11 and 13 the carbon seems to be present in form of carbonate  $\text{CO}_3$ , rather than coke. Some amounts of corrosion products are also in the solids, an extreme case is experiment 14 with 9.42 wt% Cr and 22.7 wt% Ni. Prior, this had

Table 6

EDS-analysis of solids from reactor (in wt%).

Exp. Nr.	6	7	8	9	10	11	12	13
C	81.15	71.64	89.50	68.87	79.91	74.02	81.55	47.98
O	9.12	15.05	5.91	13.68	11.04	13.87	11.25	27.28
Salt building elements								
Na	0.03	0.03	0.04		0.03	0.05		0.08
Mg	2.27	0.64	0.28	0.57	0.66	0.41	0.66	0.43
Al	0.20	0.04	0.06	0.09	0.09	0.05		0.27
Si	3.79	7.05	1.55	5.11	0.48	6.08	0.55	17.74
P	0.16	0.95	0.09	0.44	0.34	0.43	0.40	0.42
S	0.14	0.12	0.29		0.03	0.04		0.09
K	1.29	0.90	0.15	2.35	0.62	1.38	0.25	1.91
Ca	0.64	3.58	0.66	4.23	6.48	3.47	5.33	3.41
Metals								
Cr	0.22		0.42	2.41				
Fe	0.24		0.18			0.16		0.39
Ni	0.74		0.49	2.14				
Mo			0.37		0.15			
Zn				0.11		0.02		

**Table 7**  
EDS-analysis of solids from F01 (in wt%).

Exp. Nr.	5	6	7	8	9	10	11	12	13	14
C	81.38	57.24	41.68	63.27	46.91	92.17	16.29	91.60	26.05	36.45
O	8.64	21.39	24.21	24.78	22.40	4.38	41.16	4.80	37.04	18.13
Salt building elements										
Na	0.04	0.07	0.21	0.32	0.82	0.06	1.02	0.01	0.07	
Mg	0.96	3.82	0.76	0.08	1.81	0.06	0.19	0.17	0.85	2.2
Al	0.09	0.30	0.07	0.17	0.15	0.03	0.07		0.52	0.26
Si	2.19	8.24	7.07	1.02	4.86	0.08	15.78	0.32	27.65	5.13
P	0.20	1.25	0.70	0.08	0.42	0.37	0.16	0.49	0.96	0.48
S	0.20	0.06	0.42	0.59	0.26	0.10	0.13	0.17	0.16	0.34
Cl	0.06		0.53	0.11	0.47		0.35	0.04	0.12	
K	2.51	3.10	11.86	6.37	15.18	1.08	19.02	0.83	1.64	1.29
Ca	0.65	3.03	1.63			1.08	0.35	1.43	3.69	1.62
Metals										
Cr	0.36	0.14	0.86				1.28		0.15	9.42
Fe	0.29	0.35	0.44		0.81		0.18		0.90	1.98
Ni	1.63	0.15	3.19			0.24			0.20	22.70
Mo	0.79	0.69	5.98	3.07	5.89	0.34	4.02			
Zn		0.08						0.15		

been reported by Dutzi et al. who found Ni plates in the deposits [18].

As stated in Section 2.2, it is important to remove salt building elements from the system prior to the gasification reactor. There they precipitate and subsequently can cause blockage of the flow and corrosion (as can be seen in solid sample of experiment 14). The coke formation has to be reduced as well to ensure high CE and long operation. Possible measures could be the reduction of the dry matter in the feed to increase the water surplus and to reduce the contact rates of biomass molecules and intermediates that could polymerize [20,53,54]. Faster heating rates could as well be beneficial because unwanted side reactions at temperatures below 600 °C could then be reduced [34,55,56]. Kruse et al. found high concentrations of these aromatic intermediates at subcritical temperature [55].

Based on these insights, it can be concluded that plants with similar elemental composition behave similarly in the process of SCWG. Regarding the framework of CERESiS, this leads to the conclusion that the biomasses can be chosen according to their ability to remediate the grounds without the need to worry about the processing of a wide range of biomasses.

#### 4. Conclusion

In the present study the processability of different biomasses in SCWG was investigated in order to assess their potential use for preceding phytoremediation. For ten different biomasses, it was demonstrated that the macroscopic appearance, i.e. woody or grassy biomass, and the level of humidity did not influence the carbon efficiency. Carbon efficiency was  $60.3 \pm 5.1$  % for all biomasses. For all biomasses, solid deposits formed in the same part of the reaction system (containing coke, salt building elements and heavy metals), leading to plugging in most cases. The feed preparation is important in the process of SCWG. Sufficient size reduction is important to avoid plugging of the feed tubing (plugging occurred when size of biomass particles was reduced to about 1 mm with tubing with inner diameter 2.5 mm). It can be concluded that no significant differences could be determined. Thus, when pretreating the biomasses in the same way all of them could be gasified equally well and thus all of them can be considered for preceding phytoremediation. Additionally, the influence of potassium as a homogeneous catalyst (0 to 5000 ppm  $K^+$  in the feed slurry), in form of potassium hydroxide, on plants like *Panicum virgatum* was assessed. While the carbon efficiency increased from 61 to 75 % with increasing potassium concentration in the feed the amount of salt containing deposits in the reaction system did as well. Once a sufficient salt separation is installed further experiments with concentrations of potassium beyond 5000 ppm could be interesting to look at. As an additional factor, the influence of a hydrogen donor in the system was investigated in

one set of experiments conducted with 2 wt% methanol in the feed solution. While more hydrogen was present in the system during these experiments no effect on the carbon efficiency or coke formation was visible. Possibly 2 wt% of methanol was not enough to cause change. Future experiments should be conducted with higher concentrations of methanol or another hydrogen donating molecule or alternatively elemental hydrogen.

#### Funding

This research work was funded by the H2020 EU-Project CERESiS (Grant-Agreement-Nr.: 101006717).

#### Declaration of Competing Interest

The authors declare that they have no known competing financial interests or personal relationships that could have appeared to influence the work reported in this paper.

#### Data Availability

Data will be made available on request.

#### Acknowledgments

The authors would like to thank E. Hauer for the contributions to the experimental work and K. Weiss, responsible for realization of hardware and maintenance, for his contributions and for conducting part of the experiments. Special thanks to the University of Strathclyde, Universidade Federal de Goias, the University of Tuscia and the Regional Agency for Services to Agriculture and Forestry ERSAF for providing the biomasses. The authors would like to thank D. Katsourinis and A. Rentizelas for the coordination of the H2020-project CERESiS.

#### References

- [1] J.O. Nriagu, Global inventory of natural and anthropogenic emissions of trace metals to the atmosphere, *Nature* 279 (1979) 409–411, <https://doi.org/10.1038/279409A0>.
- [2] Baskar, C.; Baskar, S.; Dhillon, S. *Biomass Conversion*; Springer-Verlag Berlin Heidelberg, 2012, ISBN 978-3-642-28417-5.
- [3] CERESiS Consortium. CERESiS - Contaminated land Remediation through Energy crops for Soil improvement to liquid biofuel Strategies. Available online: <https://ceresis.eu/> (accessed on 12 December 2023).
- [4] W. Su, P. Liu, C. Cai, H. Ma, B. Jiang, Y. Xing, Y. Liang, L. Cai, C. Xia, Q.V. Le, et al., Hydrogen production and heavy metal immobilization using hyperaccumulators in supercritical water gasification, *J. Hazard. Mater.* 402 (2021) 1–9, <https://doi.org/10.1016/j.jhazmat.2020.123541>.



- [5] H. Jiang, R. Yan, C. Cai, X. Chen, F. Zhao, Z. Fan, C.C. Xu, W. Yang, Hydrothermal liquefaction of Cd-enriched *Amaranthus hypochondriacus* L. in ethanol-water co-solvent: focus on low-N bio-oil and heavy metal/metal-like distribution, *Fuel* 303 (2021) 1–9, <https://doi.org/10.1016/j.fuel.2021.121235>.
- [6] X. Zhu, F. Qian, C. Zhou, L. Li, Q. Shi, S. Zhang, J. Chen, Inherent metals of a phytoremediation plant influence its recyclability by hydrothermal liquefaction, *Environ. Sci. Technol.* 53 (2019) 6580–6586, <https://doi.org/10.1021/acs.est.9b00262>.
- [7] A. Kruse, E. Dinjus, Hot compressed water as reaction medium and reactant properties and synthesis reactions, *J. Supercrit. Fluids* 39 (2007) 362–380, <https://doi.org/10.1016/j.supflu.2006.03.016>.
- [8] F.L.P. Resende, P.E. Savage, Kinetic model for noncatalytic supercritical water gasification of cellulose and lignin, *AIChE J.* 56 (2010) 2412–2420, <https://doi.org/10.1002/aic.12165>.
- [9] M.H. Waldner, F. Krumeich, F. Vogel, Synthetic natural gas by hydrothermal gasification of biomass: Selection procedure towards a stable catalyst and its sodium sulfate tolerance, *J. Supercrit. Fluids* 43 (2007) 91–105, <https://doi.org/10.1016/j.supflu.2007.04.004>.
- [10] Q. Guan, C. Wei, P.E. Savage, Kinetic model for supercritical water gasification of algae, *Phys. Chem. Chem. Phys.* 14 (2012) 3140–3147, <https://doi.org/10.1039/c2cp23792j>.
- [11] J. Dutzi, A.A. Vadarlis, N. Boukis, J. Sauer, Comparison of experimental results with thermodynamic equilibrium simulations of supercritical water gasification of concentrated ethanol solutions with focus on water splitting, *Ind. Eng. Chem. Res.* 62 (32) (2023) 12501–12512, <https://doi.org/10.1021/acs.iecr.3c01595>.
- [12] A. Kruse, A. Funke, M. Titirici, Hydrothermal conversion of biomass to fuels and energetic materials, *Curr. Opin. Biotechnol.* 17 (2013) 515–521, <https://doi.org/10.1016/j.cbp.2013.05.004>.
- [13] R.F. Susanti, B. Veriansyah, J.-D. Kim, J. Kim, Y.-W. Lee, Continuous supercritical water gasification of isooctane: a promising reactor design, *Int. J. Hydrog. Energy* 35 (2010) 1957–1970, <https://doi.org/10.1016/j.ijhydene.2009.12.157>.
- [14] N. Boukis, I.K. Stoll, Gasification of biomass in supercritical water, challenges for the process design—lessons learned from the operation experience of the first dedicated pilot plant, *Processes* 9 (2021) 1–17, <https://doi.org/10.3390/pr9030455>.
- [15] C.R. Correa, A. Kruse, Supercritical water gasification of biomass for hydrogen production – review, *J. Supercrit. Fluids* 133 (2018) 573–590, <https://doi.org/10.1016/j.supflu.2017.09.019>.
- [16] European Commission, Directorate-General for Energy. COMMUNICATION FROM THE COMMISSION TO THE EUROPEAN PARLIAMENT, THE COUNCIL, THE EUROPEAN ECONOMIC AND SOCIAL COMMITTEE AND THE COMMITTEE OF THE REGIONS A hydrogen strategy for a climate-neutral Europe, 2020.
- [17] A.A. Vadarlis, S.D. Angeli, A.A. Lemonidou, N. Boukis, J. Sauer, Catalytic biomass gasification in supercritical water and product gas upgrading, *ChemBioEng Rev.* 10 (2023) 1–30, <https://doi.org/10.1002/cben.202300007>.
- [18] J. Dutzi, N. Boukis, J. Sauer, Process effluent recycling in the supercritical water gasification of dry biomass, *Processes* 11 (2023) 797, <https://doi.org/10.3390/pr11030797>.
- [19] C. Promdej, Y. Matsumura, Temperature effect on hydrothermal decomposition of glucose in sub- and supercritical water, *Ind. Eng. Chem. Res.* 50 (2011) 8492–8497, <https://doi.org/10.1021/ie200298c>.
- [20] P. D'Jesus, Die Vergasung von realer Biomasse in überkritischem Wasser: Untersuchung des Einflusses von Prozessvariablen und Edukteigenschaften. Dissertation; Universität Karlsruhe, Karlsruhe, Germany, 2010.
- [21] O. Yakoboylu, J. Harnick, K.G. Smit, W. Jong, Supercritical water gasification of biomass: a literature and technology overview, *energies* 8 (2015) 859–894, <https://doi.org/10.3390/en8020859>.
- [22] N. Boukis, V. Diem, W. Habicht, E. Dinjus, Methanol reforming in supercritical water, *Ind. Eng. Chem. Res.* 42 (2003) 728–735, <https://doi.org/10.1021/ie020557i>.
- [23] J.B. Gadhe, R.B. Gupta, Hydrogen production by methanol reforming in supercritical water: suppression of methane formation, *Ind. Eng. Chem. Res.* 44 (2005) 4577–4585, <https://doi.org/10.1021/ie049268f>.
- [24] W. Habicht, N. Boukis, G. Franz, E. Dinjus, Investigation of nickel-based alloys exposed to supercritical water environments, *Microchim. Acta* 145 (2004) 57–62, <https://doi.org/10.1007/s00604-003-0127-9>.
- [25] R.E. Zeebe, D. Wolf-Gladrow, *CO<sub>2</sub> in seawater: equilibrium, kinetics, isotopes*. Elsevier Science, 2001. ISBN 9780444509468.
- [26] A. Hart, Modern techniques to minimize catalyst deactivation due to coke deposition in catalytic upgrading of heavy oil in situ processes, *Pet. Chem.* 62 (2022) 714–731, <https://doi.org/10.1134/S0965544122020189>.
- [27] J. Chumpoo, P. Prasassarakich, Bio-oil from hydro-liquefaction of bagasse in supercritical ethanol, *Energy Fuels* 24 (2010) 2071–2077, <https://doi.org/10.1021/ef901241e>.
- [28] A. Hammerschmidt, N. Boukis, U. Galla, E. Dinjus, B. Hitzmann, Conversion of yeast by hydrothermal treatment under reducing conditions, *Fuel* 90 (2011) 3424–3432, <https://doi.org/10.1016/j.fuel.2011.06.052>.
- [29] M. Watanabe, S. Kato, S. Ishizeki, H. Inomata, R.L. Smith Jr, Heavy oil upgrading in the presence of high density water: basic study, *J. Supercrit. Fluids* 53 (2010) 48–52, <https://doi.org/10.1016/j.supflu.2009.11.013>.
- [30] A. Kruse, Supercritical water gasification, *Biofuels, Bioprod., Bioref.* 2 (2008) 415–437, <https://doi.org/10.1002/bbb>.
- [31] A. Chuntanapum, Y. Matsumura, Char formation mechanism in supercritical water gasification process: a study of model compounds, *Ind. Eng. Chem. Res.* 49 (2010) 4055–4062, <https://doi.org/10.1021/ie901346h>.
- [32] P. D'Jesus, N. Boukis, B. Kraushaar-Czarnetski, E. Dinjus, Gasification of corn and clover grass in supercritical water, *Fuel* 85 (2006) 1032–1038, <https://doi.org/10.1016/j.fuel.2005.10.022>.
- [33] G. Akgül, A. Kruse, Influence of salts on the subcritical water-gas shift reaction, *J. Supercrit. Fluids* 66 (2012) 207–214, <https://doi.org/10.1016/j.supflu.2011.10.009>.
- [34] A. Sinag, A. Kruse, J. Rathert, Influence of the heating rate and the type of catalyst on the formation of key intermediates and on the generation of gases during hydrolysis of glucose in supercritical water in a batch reactor, *Ind. Eng. Chem. Res.* 43 (2004) 502–508, <https://doi.org/10.1021/ie030475r>.
- [35] A. Sinag, A. Kruse, V. Schwarzkopf, Key compounds of the hydrolysis of glucose in supercritical water in the presence of K<sub>2</sub>CO<sub>3</sub>, *Ind. Eng. Chem. Res.* 42 (2003) 3516–3521, <https://doi.org/10.1021/ie030079r>.
- [36] Z. Zhu, S.S. Toor, L.A. Rosendahl, D. Yu, G. Chen, Influence of alkali catalyst on product yield and properties via hydrothermal liquefaction of barley straw, *Energy* 80 (2015) 284–292, <https://doi.org/10.1016/j.energy.2014.11.071>.
- [37] H. Weingärtner, E.U. Franck, Überkritisches Wasser als Lösungsmittel, *Angew. Chem.* 117 (2005) 2730–2752, <https://doi.org/10.1002/ange.200462468>.
- [38] V. Valyashko, Phase behaviour in binary and ternary water-salt systems at high temperatures and pressures, *Pure Appl. Chem.* 69 (1997) 2271–2280, <https://doi.org/10.1351/PAC199769112271>.
- [39] M. Schubert, J.W. Regler, F. Vogel, Continuous salt precipitation and separation from supercritical water. Part 1: type 1 salts, *J. Supercrit. Fluids* 52 (2010) 99–112, <https://doi.org/10.1016/j.supflu.2009.10.002>.
- [40] A. Kruse, Hydrothermal biomass gasification, *J. Supercrit. Fluids* 47 (2009) 391–399, <https://doi.org/10.1016/j.supflu.2008.10.009>.
- [41] R. Singh, B.B. Krishna, J. Kumar, T. Bhaskar, Opportunities for utilization of non-conventional energy sources for biomass pretreatment, *Bioresour. Technol.* 199 (2016) 398–407, <https://doi.org/10.1016/j.biortech.2015.08.117>.
- [42] P. Kumar, D.M. Barrett, M.J. Delwiche, P. Stoeve, Methods for pretreatment of lignocellulosic biomass for efficient hydrolysis and biofuel production, *Ind. Eng. Chem. Res.* 48 (2009) 3713–3729, <https://doi.org/10.1021/ie801542g>.
- [43] Z. Rastegar, A. Ghaemi, CO<sub>2</sub> absorption into potassium hydroxide aqueous solution: experimental and modeling, *Heat. Mass Transf.* 58 (2022) 365–381, <https://doi.org/10.1007/s00231-021-03115-9>.
- [44] R.D. Gonzales, H. Miura, Methanation and Fischer-Tropsch studies on potassium-promoted silica-supported Ru catalysts, *J. Catal.* 77 (1982) 338–347, [https://doi.org/10.1016/0021-9517\(82\)90177-4](https://doi.org/10.1016/0021-9517(82)90177-4).
- [45] Schubert, M. Catalytic hydrothermal gasification of biomass - Salt recovery and continuous gasification of glycerol solutions. Dissertation; Eidgenössische Technische Hochschule Zürich, Zurich, Switzerland, 2010.
- [46] F.J. Armellini, *Phase equilibria and precipitation phenomena of sodium chloride and sodium sulfate in sub- and supercritical water*. Dissertation, Massachusetts Institute of Technology, Cambridge, USA, 1993.
- [47] M. Hodes, P.A. Marrone, G.T. Hong, K.A. Smith, J.W. Tester, Salt precipitation and scale control in supercritical water oxidation—Part A. Fundamentals and research, *J. Supercrit. Fluids* 29 (2004) 265–288, [https://doi.org/10.1016/S0896-8446\(03\)00093-7](https://doi.org/10.1016/S0896-8446(03)00093-7).
- [48] P. Kritzer, N. Boukis, E. Dinjus, Factors controlling corrosion in high-temperature aqueous solutions. A contribution to the dissociation and solubility data influencing corrosion processes, *J. Supercrit. Fluids* 15 (1999) 205–227, [https://doi.org/10.1016/S0896-8446\(99\)00009-1](https://doi.org/10.1016/S0896-8446(99)00009-1).
- [49] Boukis, N.; Habicht, W.; Hauer, E.; Weiss, K.; Dinjus, E. Corrosion behavior of Ni-base alloy 625 in supercritical water containing alcohols and potassium hydrogen carbonate. In the Proceedings of EUROCORR 2007 the European Corrosion Congress, Freiburg in Breisgau, Germany, 9–13. September 2007.
- [50] Boukis, N.; Galla, U.; Müller, H.; Dinjus, E. Biomass Gasification in Supercritical Water. Experimental progress achieved with the VERENA pilot plant. In Proceedings of 15th European Biomass Conference & Exhibition, Berlin, Germany, 7–11 May 2007.
- [51] D. Castello, A. Kruse, L. Fiori, Supercritical water gasification of glucose/phenol mixtures as model compounds for ligno-cellulosic biomass, *Chem. Eng. Trans.* 37 (2014) 193–198, <https://doi.org/10.3303/CET1437033>.
- [52] M. Yan, Y. Liu, Y. Song, A. Xu, G. Zhu, J. Jiang, D. Hantoko, Comprehensive experimental study on energy conversion of household kitchen waste via integrated hydrothermal carbonization and supercritical water gasification, *Energy* 242 (2022), <https://doi.org/10.1016/j.energy.2021.123054>.
- [53] J.A. Okolie, R. Rana, S. Nanda, A.K. Dalai, J.A. Kozinski, Supercritical water gasification of biomass: a state-of-the-art review of process parameters, reaction mechanisms and catalysis, *Sustain. Energy Fuels* 3 (2019) 578–598, <https://doi.org/10.1039/c8se00565f>.
- [54] S. Nanda, S.N. Reddy, H.N. Hunter, A.K. Dalai, J.A. Kozinski, Supercritical water gasification of fructose as a model compound for waste fruits and vegetables, *J. Supercrit. Fluids* 104 (2015) 112–121, <https://doi.org/10.1016/j.supflu.2015.05.009>.
- [55] A. Kruse, M. Faquir, Hydrothermal biomass gasification – effects of salts, backmixing, and their interaction, *Chem. Eng. Technol.* 30 (6) (2007) 749–754, <https://doi.org/10.1002/ceat.200600409>.
- [56] Y. Matsumura, M. Harada, K. Nagata, Y. Kikuchi, Effect of heating rate of biomass feedstock on carbon gasification efficiency in supercritical water gasification, *Chem. Eng. Commun.* 193 (2006) 649–659, <https://doi.org/10.1080/00986440500440157>.